Direct determination of the energy of the first excited fine-structure level in Ba^{6+}

N. Kimura,[1,2,*] R. Kodama,[3] K. Suzuki,[3] S. Oishi,[3] M. Wada,[4] K. Okada,[1] N. Ohmae,[5,6] H. Katori,[5,6,7] and N. Nakamura[3]

[1]*Department of Physics, Sophia University, 7-1 Kioicho, Chiyoda, Tokyo 102-8554, Japan*

[2]*RIKEN Nishina Center, Saitama 351-0198, Japan*

[3]*Institute for Laser Science, The University of Electro-Communications, Tokyo 182-8585, Japan*

[4]*Wako Nuclear Science Center, Inst. of Particle and Nuclear Studies, High Energy Accelerator Research Organization (KEK), Saitama 351-0198, Japan*

[5]*Quantum Metrology Laboratory, RIKEN, Saitama 351-0198, Japan*

[6]*RIKEN Center for Advanced Photonics, Saitama 351-0198, Japan*

[7]*Department of Applied Physics, The University of Tokyo, Tokyo 113-8656, Japan*

(Received 3 September 2019; published 21 November 2019)

We present an experimental observation of the visible magnetic dipole transition between the fine structure levels in the ground term of Ba^{6+} ($5s^2 5p^2$: $^3P_0 - {}^3P_1$) with a compact electron beam ion trap. The wave number in vacuum of the transition is determined to be 15505.506(37) cm^{-1} by simultaneously observing the reference lines of neutral Ne. The present measurement reduces the uncertainty in the previously reported value obtained from observation of the electric dipole transitions to the ground terms in the extreme ultraviolet range [Phys. Scr. **46**, 403 (1992)].

DOI: 10.1103/PhysRevA.100.052508

I. INTRODUCTION

Visible transitions of highly charged ions (HCIs) can be used in various applications. For instance, observation and analysis of visible emissions from highly charged W ions in ITER plasma are considered to be useful for understanding the plasma condition [1]. Spectroscopic studies of highly charged W ions have thus been widely performed to expand the reference data for the ITER plasma diagnosis [2–4]. On the other hand, experimental spectral data of visible transitions in highly charged Fe ions have been applied to the studies of the solar corona [5,6]. In addition, precision measurements of visible transitions in highly charged ions can provide important benchmarks for theoretical studies, such as the verification of QED effects [7], many-body recoil effects [8], and g-factor calculations of HCIs [9].

In recent years, several visible transitions in HCIs have also attracted attention as a candidate for a new type of atomic clock that can evaluate fundamental physics [10,11]. Since transitions in HCIs are relatively insensitive to external perturbation fields compared to those in neutral and singly ionized atoms, it is possible to construct an optical atomic clock with an accuracy higher than current optical clocks. Additionally, HCI clock transitions have the potential to reveal possible time variation of the fine-structure constant α as the strong relativistic effect brought about by the huge effective nuclear charge in HCIs gives high sensitivity to the variation of α. Recently, Schmöger *et al.* demonstrated Coulomb crystallization of highly charged Ar ions in a linear radio-frequency (rf) trap with the aim towards the precision spectroscopy of HCIs [12,13]. Their successful results accelerated the realization of high-precision laser spectroscopy of HCIs. To date, several experimental and theoretical efforts have been made to use $4f$-$5s$ transitions in heavy HCIs that fall in the optical range for electron shelving laser spectroscopy or quantum logic spectroscopy [14–19]. However, such laser spectroscopy schemes are not easy due to the complicated energy levels arising from open $4f$ shell structures. Alternatively, we recently proposed to use magnetic dipole (M1) transitions between the fine-structure splitting in the ground term for simplified Doppler-free spectroscopy using direct observation of laser-induced fluorescence (LIF) [20]. However, such transitions with small Einstein A coefficient are not easy to observe by LIF, because of the small number of fluorescence photons. Therefore, the transition wavelength has to be determined as accurately as possible in advance for searching the resonant wavelength with laser spectroscopy. Some transition energies of these candidates have already been predicted theoretically [14,21–23], and some of them have been identified experimentally [3,7,19,20,24]. In particular, ions having no hyperfine structure, such as Ar^{13+}, Ba^{6+}, Ba^{7+}, Ba^{11+}, Ce^{9+}, W^{7+}, W^{13+}, W^{27+}, and Er^{21+}, are promising candidates, because a closed optical transition cycle can be maintained with only one laser.

According to the above-mentioned motivations, we have studied visible transitions in HCIs with a compact electron beam ion trap (EBIT) called CoBIT [25]. In our previous experiments [3,4,19,26], we used reference spectra from standard light sources placed at the outside of CoBIT for the wavelength determinations of the observed HCI transitions. The Ne lamp spectra were measured before and after the observation of HCI transitions, and they were adopted for the wavelength determinations only when no drift was observed.

*Present address: Atomic, Molecular and Optical Physics Laboratory, RIKEN, Wako, Saitama, 351-0198, Japan; naoki.kimura@riken.jp

Nevertheless, we had to adopt large systematic uncertainties, which were typically about 2.0 cm^{-1}, in consideration of the differences in the light source position and the measurement timing. In order to reduce the systematic uncertainty, it is desirable to simultaneously observe an objective HCI line and well-known reference lines emitted from the same position. Such a calibration method has been applied for a few EBIT measurements so far [27]. For example, in the precision wavelength measurement of Ar^{13+}, well-known neutral Ar and Ar^{+} transitions were simultaneously observed by introducing three times the usual amount of Ar gas [7,27,28]. Recently, in the visible spectroscopy of Ba^{7+}, we demonstrated calibration with well-known Ar^{+} transitions simultaneously excited in CoBIT [20].

Here we report the direct observation and wavelength determination of the visible M1 transition between the ground-term fine-structure levels of Ba^{6+} using CoBIT with a visible spectrometer. For accurate wavelength calibration, we utilized simultaneously emitted reference lines from introduced neutral Ne.

II. EXPERIMENT

In the present experiments, highly charged Ba ions were generated with CoBIT [25]. The details of CoBIT with a visible spectrometer are described in a previous paper [26]. Briefly, CoBIT consists of three elements: an electron gun, a drift tube (DT) surrounded by a high-critical-temperature superconducting coil, and an electron collector. The DT is further divided into three parts (DT1, DT2, DT3) for form an axial trapping potential. The electrons emitted from the electron gun pass through the inside of the DT and reach the electron collector. In the DT, the electron beam is compressed by the axial magnetic field (Typ. 0.08 T) produced by the coil. The space charge of the electron beam forms the trap potential in the radial direction. Highly charged ions are generated by the successive ionization of the trapped ions. The electron beam energy is determined by the potential difference between the cathode of the electron gun and the trap region.

The background gas pressure of the CoBIT chamber was about 1×10^{-8} Pa throughout the present measurements. Ba was introduced by the evaporation of the cathode material (BaO) of the electron gun, following our previous papers [26,29]. In order to observe emission from neutral Ne simultaneously, Ne gas was separately introduced into the trap region through a variable leak valve. The Ne gas pressure was monitored with a cold cathode gauge (Pfeiffer vacuum IKR270) located at the outside of the DT and the measured pressure was calibrated by the sensitivity factor of Ne ($\times 4.1$).

Visible emission spectra were observed with a Peltier-cooled, back illuminated charge coupled device (CCD) camera (Andor iDus 416) connected to a Czerny-Turner type visible spectrometer (Jobin Yvon HR320) with a 1200 gr/mm grating blazed at 400 nm. The exposure time was typically 10 min per one measurement. The background measurements were performed under the electron-beam off condition beforehand in order to distinguish the emission spectra from the background structure of the stray light from the cathode. The wavelengths of the observed spectra were calibrated by Ne emission spectra whose wavelengths are accurately known [30] as described in detail below.

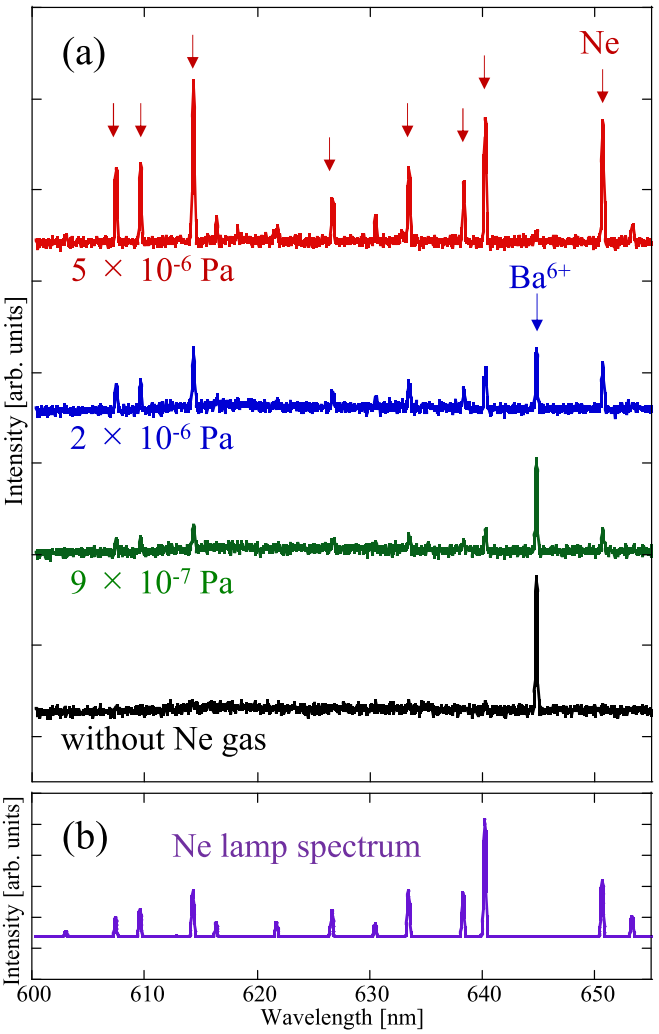

FIG. 1. (a) Introduced Ne gas pressure dependence of visible emission spectra of Ba^{6+} and Ne. The introduced Ne gas pressure measured in the room temperature region of the CoBIT chamber are shown under each spectrum. The emission peaks of the neutral Ne atoms and the Ba^{6+} ions are indicated by the red arrows and the blue arrows, respectively. (b) External Ne lamp spectrum observed before the measurement of (a).

III. RESULTS AND DISCUSSION

Figure 1(a) shows the visible emission spectra of Ba^{6+} and Ne at several different Ne gas pressures after the subtraction of the background structures. These spectra were observed at an electron beam energy of 70 eV. The wavelength scale was calibrated with the Ne lamp spectrum shown in Fig. 1(b). In the condition without Ne gas loading, an emission line due to Ba was observed around 645 nm. We assigned this peak as the M1 transition between fine-structure levels ($J = 0$–1) in the ground term (^3P) of Ba^{6+} by comparison with the energy levels determined from the previous observations of the electric dipole transitions to the ground terms in the extreme ultraviolet (EUV) range [31]. As Ne gas pressure

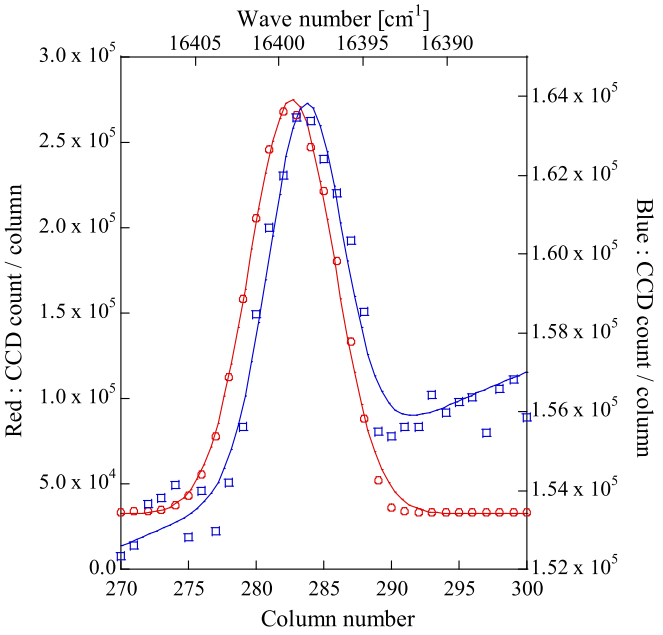

FIG. 2. Comparison of the peak position between the external Ne lamp (red) and the internal emission from the CoBIT trap region for the neutral Ne line at 610 nm. The corresponding wave number calibrated by the Ne lamp spectrum is indicated on the upper side of the graph. The left vertical axis is for the external lamp (red) and the right axis for the internal emission (blue).

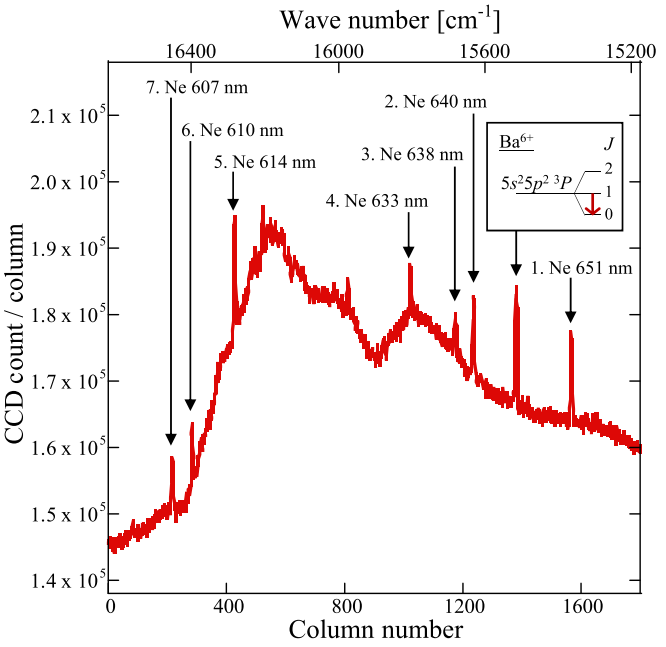

FIG. 3. Typical visible emission spectrum of Ba^{6+} and neutral Ne without background subtraction as a function of column number. The corresponding wave number was scaled by the Ne lamp spectrum.

increases, the intensity of the Ba^{6+} peak decreases possibly due to charge exchange reactions between the trapped Ba ions and introduced Ne. On the other hand, emission lines of neutral Ne increased with the Ne gas pressure. The accurate wavelengths of these Ne lines are already well known and compiled in the NIST database [32]. The uncertainty of these wavelengths is 0.1 ppm or less; thus, these Ne peaks are suitable for the precise wavelength calibration of the Ba^{6+} transition. The appropriate gas pressure where the Ne reference peaks and the Ba^{6+} peak can be simultaneously observed was experimentally determined to be 2×10^{-6} Pa.

The advantages of this calibration method are summarized as follows. First, the systematic uncertainties caused by a difference in the position between the trapped HCIs and the reference source are eliminated. Second, it is not necessary to consider the thermal and mechanical drifts due to the difference in the measurement timing between the calibration lines and the objective line. Figure 2 shows the Ne emission line at 610 nm obtained from the internal source and the external lamp source. As seen in this example, the difference in the peak position can sometimes be as large as about one column, which corresponds to about 1 cm^{-1} while the difference was confirmed to be typically much smaller than this example.

Figure 3 shows the typical spectrum with Ba^{6+} and neutral Ne lines without background subtraction. The horizontal and vertical axes are the column position on the CCD sensor and the number of electron counts created in the CCD sensor at each column position, respectively. Although a large background structure appeared due to the stray light from the cathode, we confirmed that there was no peculiar structure around the Ba^{6+} and reference Ne peaks. The wavelength of the Ba^{6+} line was determined by the following procedure. All analyses were performed based on the wave number in vacuum. First, the relative column position of each peak was determined from peak fitting. A Gaussian function with a linear background was fitted to each observed peak weighted by the inverse of the number of electron counts. The peak shift and broadening due to Zeeman, Stark, and collisional effects were estimated to be negligibly small compared with the uncertainty caused by the optical system in the present experimental conditions. In order to take correlations between every peak into account, all the fitting functions were fitted to all peaks at the same time. The peak position parameter in each Gaussian function was described as a relative column position with respect to the Ba^{6+} peak position. Figure 4(a) shows the relative column position of the Ne lines as a function of the wave number in vacuum. The wave numbers of the Ne peaks were quoted from the literature [30]. Since wavelength-dispersive spectrometers generally have a nonlinearity between the position of dispersed light and the wavelength, an empirically determined cubic polynomial [solid line in Fig. 4(a)] was used as a fitting function [7,33]. The relative position uncertainties of the calibration peaks were included as weights for the fitting. The wave number of the Ba^{6+} transition was obtained by calculating the wave number (x axis) on the calibration curve at the position where the column position (y axis) is 0. Figure 4(b) shows the deviation of the Ne peak positions from the fitted calibration of Fig. 4(a) as a function of wave number. The error bars represent the peak fitting error of relative column position. The solid blue lines indicate the confidence interval (1σ). We adopt the confidence interval at the origin of the column position as the uncertainty of one measurement. Typically, the full-width-at-half-maximum and

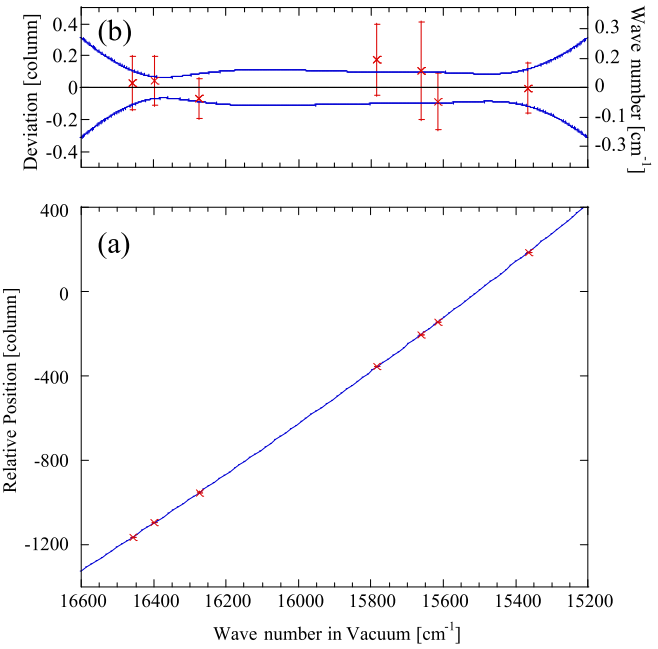

FIG. 4. (a) Relation between the literature values [30] of the observed Ne peak wave numbers and the relative column position in the CCD sensor with respect the Ba^{6+} peak. The blue line is the calibration curve obtained by fitting with a cubic polynomial function. (b) Residual plots of each calibration Ne line from the calibration curve. The right vertical axis shows the corresponding wave number. The interval between the blue lines shows the range-of-confidence interval (1σ) of the calibration curve.

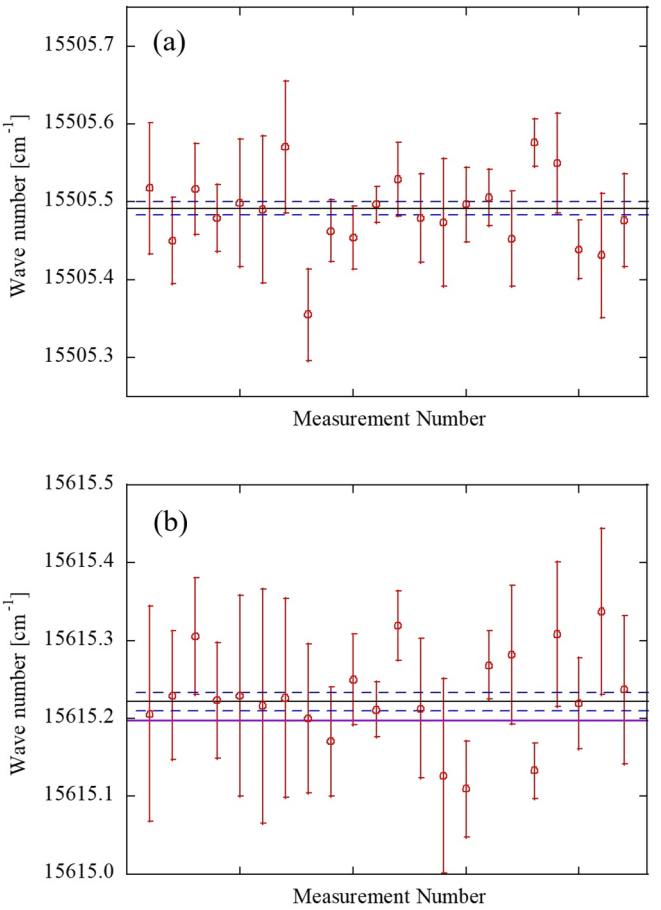

FIG. 5. Experimental wave number (in vacuum) for (a) $^3P_0$-$^3P_1$ in Ba^{6+} determined with the seven calibration lines in Fig. 3, and for (b) the Ne No. 2 line in Fig. 3 determined with the six calibration lines without No. 2 (see text for details). The black solid line is the weighted average of this data set. The blue dashed lines show the range of the standard error. The purple solid line is the literature value [30].

the uncertainty obtained by this method were 6 cm^{-1} and 0.04 cm^{-1}, respectively, for the Ba^{6+} line.

We repeated this measurement 22 times and obtained the results as shown in Fig. 5(a). The renormalized error bars (1σ), which were estimated to fit to the dispersion of the data, are shown in the figure because the uncertainty of each measurement estimated from the confidence interval of the calibration curve was smaller than the dispersion of the data set. The weighted average and the standard error of the data set shown in Fig. 5(a) are 15505.492 cm^{-1} and 0.010 cm^{-1}, respectively. In order to evaluate the systematic uncertainty, we determined the wave number of the well-known neutral Ne line indicated by "No. 2" in Fig. 3 using other calibration lines. Figure 5(b) shows the wave number of the Ne line No. 2, which was determined using the same data set. The literature value of this Ne line is shown as the solid purple line [30]. As seen in the figure, the deviation between the experimental and literature values is larger than the standard error, which indicates that systematic errors exist in the present measurements. In the present experiment, the error factors derived from the difference in the emission source position or the measurement timing should have been eliminated by simultaneously observing the reference Ne lines from CoBIT. Therefore, we consider that the deviation was caused by the invalidity of the use of a polynomial function for the conversion from column position to wave number. As the Ne line No. 2 is the closest to the Ba^{6+} line, we consider that the systematic uncertainty of the Ba^{6+} peak can be reasonably evaluated by that of the Ne line No. 2. The systematic uncertainty was thus estimated to be 0.025 cm^{-1} from the difference between the measured [the black line in Fig. 5(b)] and the literature [the purple line in Fig. 5(b)] values. The calibration curve used in the wave number determination of the Ne No. 2 line gives 15505.506(12) cm^{-1} for the Ba^{6+} line, which is slightly different from the value [15505.492(10) cm^{-1}] obtained by the calibration curve including the Ne No. 2 line as a reference. However, since the difference is smaller than the estimated systematic uncertainty, we finally adopt the value obtained with the calibration curve used in the wave number determination of the Ne No. 2 line as listed in Table I. The uncertainty in the present work is given by the sum of the standard error and the systematic uncertainty. The previous theoretical study by Safronova *et al.* [21] was carried out by the combined approach of the configuration interaction (CI) method and the linearized coupled-cluster (CC) method. The experimental value by Tauheed *et al.* [31] was indirectly obtained from the observations of the electric dipole transitions to the ground terms in the EUV range. The uncertainty of the previous experiment was not given in the original paper, but the NIST database tabulates this value as

TABLE I. Summary of the present work and the previous studies. The wave number k in vacuum of the transition between the fine structure splitting of $5s^2 5p^2\ ^3P_0$-$^3P_1$ in Ba^{6+} is given.

	Th. or Expt.	k [cm^{-1}]	Uncertainty
Safronova [21]	Th.	15425	
Tauheed [31,32]	Expt. (indirect)	15506.6	0.8
This work	Expt. (direct)	15505.506	0.037

15506.6 ± 0.8 cm^{-1}. The present and the previous values show reasonable agreement considering the errors represent 1σ, but the uncertainty has been much reduced by a factor larger than 20.

IV. SUMMARY AND OUTLOOK

In summary, we observed the visible emission spectra of trapped Ba^{6+} ions with a compact electron beam ion trap. We demonstrated the wavelength calibration with neutral Ne lines simultaneously observed with the objective Ba^{6+} line by introducing Ne buffer gas. The wavelength of the magnetic dipole transitions between the ground-term fine-structure levels of Ba^{6+} was thus precisely determined. The present measurement successfully reduced the uncertainty in the energy of the first excited fine structure level, which was previously determined from the observation of the electric dipole transitions to the ground state in the EUV range.

The wavelength of the Ba^{6+} line determined in the present study is also useful for our next experiment. Recently, we started to develop an experimental setup for HCI clocks in RIKEN and plan to perform Doppler-free spectroscopy of cold Ba HCIs using a sympathetic cooling method with laser cooled Be^+ ions [34]. Ba^{6+} is a candidate for the first target in this experiment. We are preparing a laser based on the wavelength measured in this paper to observe laser-induced fluorescence from sympathetically crystallized Ba^{6+} ions.

ACKNOWLEDGMENTS

This work is supported by RIKEN Pioneering Project Funding and Grant-in-Aid for JSPS Research Fellow (No. 17J05087). We would like to thank Dr. Kiattichart Chartkunchand for the proofreading of the manuscript.

[1] Y. Ralchenko, Plasma Fusion Res. **8**, 2503024 (2013).
[2] A. Komatsu, J. Sakoda, M. Minoshima, H. A. Sakaue, X.-B. Ding, D. Kato, I. Murakami, F. Koike, and N. Nakamura, Plasma Fusion Res. **7**, 1201158 (2012).
[3] Y. Kobayashi, K. Kubota, K. Omote, A. Komatsu, J. Sakoda, M. Minoshima, D. Kato, J. Li, H. A. Sakaue, I. Murakami, and N. Nakamura, Phys. Rev. A **92**, 022510 (2015).
[4] M. Mita, H. A. Sakaue, D. Kato, I. Murakami, and N. Nakamura, Atoms **5**, 13 (2017).
[5] P. Beiersdorfer, E. Träbert, and E. H. Pinnington, Astrophys. J. **587**, 836 (2003).
[6] G. Brenner, J. R. Crespo Lopez-Urrutia, S. Bernitt, D. Fischer, R. Ginzel, K. Kubicek, V. Mackel, P. H. Mokler, M. C. Simon, and J. Ullrich, Astrophys. J. **703**, 68 (2009).
[7] I. Draganic, J. R. CrespoLopez-Urrutia, R. DuBois, S. Fritzsche, V. M. Shabaev, R. S. Orts, I. I. Tupitsyn, Y. Zou, and J. Ullrich, Phys. Rev. Lett. **91**, 183001 (2003).
[8] R. SoriaOrts, Z. Harman, J. R. Lopez-Urrutia, A. N. Artemyev, H. Bruhns, A. J. GonzalezMartinez, U. D. Jentschura, C. H. Keitel, A. Lapierre, V. Mironov, V. M. Shabaev, H. Tawara, I. I. Tupitsyn, J. Ullrich, and A. V. Volotka, Phys. Rev. Lett. **97**, 103002 (2006).
[9] R. Soria Orts, J. R. Crespo López-Urrutia, H. Bruhns, A. J. Gonzalez Martinez, Z. Harman, U. D. Jentschura, C. H. Keitel, A. Lapierre, H. Tawara, I. I. Tupitsyn, J. Ullrich, and A. V. Volotka, Phys. Rev. A **76**, 052501 (2007).
[10] J. C. Berengut, V. A. Dzuba, and V. V. Flambaum, Phys. Rev. Lett. **105**, 120801 (2010).
[11] M. G. Kozlov, M. S. Safronova, J. R. Crespo López-Urrutia, and P. O. Schmidt, Rev. Mod. Phys. **90**, 045005 (2018).
[12] L. Schmöger, O. O. Versolato, M. Schwarz, M. Kohnen, A. Windberger, B. Piest, S. Feuchtenbeiner, J. Pedregosa-Gutierrez, T. Leopold, P. Micke, A. K. Hansen, T. M. Baumann, M. Drewsen, J. Ullrich, P. O. Schmidt, and J. R. Crespo López-Urrutia, Science **347**, 1233 (2015).
[13] L. Schmöger, M. Schwarz, T. M. Baumann, O. O. Versolato, B. Piest, T. Pfeifer, J. Ullrich, P. O. Schmidt, and J. R. Crespo Lopez-Urrutia, Rev. Sci. Instrum. **86**, 103111 (2015).
[14] J. C. Berengut, V. A. Dzuba, V. V. Flambaum, and A. Ong, Phys. Rev. Lett. **106**, 210802 (2011).
[15] U. I. Safronova, V. V. Flambaum, and M. S. Safronova, Phys. Rev. A **92**, 022501 (2015).
[16] V. A. Dzuba, V. V. Flambaum, and H. Katori, Phys. Rev. A **91**, 022119 (2015).
[17] A. Windberger, J. R. Crespo López-Urrutia, H. Bekker, N. S. Oreshkina, J. C. Berengut, V. Bock, A. Borschevsky, V. A. Dzuba, E. Eliav, Z. Harman, U. Kaldor, S. Kaul, U. I. Safronova, V. V. Flambaum, C. H. Keitel, P. O. Schmidt, J. Ullrich, and O. O. Versolato, Phys. Rev. Lett. **114**, 150801 (2015).
[18] T. Nakajima, K. Okada, M. Wada, V. A. Dzuba, M. S. Safronova, U. I. Safronova, N. Ohmae, H. Katori, and N. Nakamura, Nucl. Instrum. Meth. Phys. Res. B **408**, 118 (2017).
[19] S. Murata, T. Nakajima, M. S. Safronova, U. I. Safronova, and N. Nakamura, Phys. Rev. A **96**, 062506 (2017).
[20] N. Kimura, R. Kodama, K. Suzuki, S. Oishi, M. Wada, K. Okada, N. Ohmae, H. Katori, and N. Nakamura, Plasma Fusion Res. **14**, 1201021 (2019).
[21] M. S. Safronova, V. A. Dzuba, V. V. Flambaum, U. I. Safronova, S. G. Porsev, and M. G. Kozlov, Phys. Rev. A **90**, 042513 (2014).
[22] M. S. Safronova, V. A. Dzuba, V. V. Flambaum, U. I. Safronova, S. G. Porsev, and M. G. Kozlov, Phys. Rev. A **90**, 052509 (2014).
[23] D. K. Nandy and B. K. Sahoo, Phys. Rev. A **94**, 032504 (2016).
[24] Z. Fei, R. Zhao, Z. Shi, J. Xiao, M. Qiu, J. Grumer, M. Andersson, T. Brage, R. Hutton, and Y. Zou, Phys. Rev. A **86**, 062501 (2012).

[25] N. Nakamura, H. Kikuchi, H. A. Sakaue, and T. Watanabe, Rev. Sci. Instrum. **79**, 063104 (2008).
[26] J. Sakoda, A. Komatsu, H. Kikuchi, and N. Nakamura, Phys. Scr. T **144**, 014011 (2011).
[27] J. R. Crespó Lopez-Urrutia, P. Beiersdorfer, K. Widmann, and V. Decaux, Can. J. Phys., **80**, 1687 (2002).
[28] I. Draganić, J. R. Crespó Lopez-Urrutia, R. DuBois, R. Soria Orts, V. M. Shabaev, S. Fritzsche, Y. Zou, and J. Ullrich, AIP Conf. Proc. **740**, 364 (2004).
[29] S. Ali and N. Nakamura, Nucl. Instrum. Methods Phys. Res. Sect. B **408**, 122 (2017).
[30] W. F. Meggers and C. J. Humphreys, J. Res. Natl. Bur. Stand. (U. S.) **13**, 293 (1934).
[31] A. Tauheed and Y. N. Joshi, Phys. Scr. **46**, 403 (1992).
[32] https://www.nist.gov/pml/atomic-spectra-database
[33] S. T. Wollman and P. W. Bohn, Appl. Spec. **47**, 125 (1993).
[34] N. Kimura, K. Okada, N. Nakamura, N. Ohmae, K. Katori, and M. Wada, RIKEN Accel. Prog. Rep. **50**, 202 (2017).